

Application of a Cost-Effective 3-D Creep Analysis to a PCRV

I.G. Smith, J.S. Bateman

*Department of Industry,
National Engineering Laboratory, East Kilbride, Glasgow,
Scotland G75 0QU, United Kingdom*

G.L. England

*Department of Civil Engineering, University of London,
King's College, Strand, London WC2R 2LS, United Kingdom*

J.S. MacLeod

*Nuclear Installations Inspectorate,
Health & Safety Executive, Thames House North, Millbank,
London SW1P 4QJ, United Kingdom*

S U M M A R Y

This paper presents an economic analysis for the determination of time-dependent stresses in three-dimensional heated concrete structures. Current methods, based on the time-stepping approach, are very expensive when a large three-dimensional problem is considered.

A direct method of solution, based on a minimum power principle, which does not require intermediate solutions at many small intervals of time has been developed. The method has been used in conjunction with a standard stiffness approach finite element program, in the time-dependent analysis of a PCRV.

Comparative solutions are presented for three different degrees of approximation, and it is concluded that a small number of easily selected basic stress distributions can generate an acceptable creep solution at low cost.

NOTE: The views expressed in this paper are those of the authors and do not necessarily reflect those of the Health and Safety Executive.

1 INTRODUCTION

In prestressed concrete structures subjected to spatially non-uniform temperatures, the internal stresses change with time and undergo redistribution due to temperature-dependent creep. The redistribution tends to a limiting, or steady-state (SSL), condition whenever loads and temperatures are time-invariant and these steady-state stresses may be calculated directly when required, England [1].

A nuclear reactor prestressed containment vessel is an example of a structure where these conditions apply, and for which the time-dependent stresses vary considerably from the stress distribution at the commissioning stage. Because conventional thermo-elastic stiffness analysis cannot be used reliably to predict the state of stress after commissioning, separate calculations must be performed whenever the detailed nature of the transient creep phase is required.

Historically, creep analyses of nuclear reactor containment vessels have been performed using time-step approaches. These have necessitated the use of many small time-steps to retain accuracy of solution. In consequence, three-dimensional analyses of reactor vessels have been performed on a limited scale only due to prohibitively high computer processing costs. Occasionally a structure could be idealized to a simpler axisymmetric or two-dimensional model to reduce costs. However, there are many situations where a two-dimensional analysis would be inappropriate. A three-dimensional solution is then essential.

The purpose of this paper is to illustrate an alternative approach which is both economic and direct (ie non time-step) to the solution of the non-homogeneous three-dimensional creep problem. This method is based upon an optimization procedure using a minimum power principle and has been demonstrated for the axisymmetric analysis of a containment vessel, England and MacLeod [2]. A three-dimensional program, based on this work, has been developed and tested at NEL. It has been used to analyse a geometrically asymmetric nominal containment vessel for a nuclear reactor system.

2 PRESTRESSED CONCRETE CONTAINMENT VESSEL

The nominal vessel considered, shown in Fig. 1, has approximate dimensions of 38 m in height, 17.8 m outer radius and 14.4 m inner radius. The loads shown here have been taken to be constant in time. Not shown, but included in the analysis are the gravity effects of the structural mass. The effects of the liner were not considered. The inner and outer surface temperatures were held at 65 and 20°C respectively throughout the analysis. A more detailed description of the internal temperature distribution is given by Smith [3]. The material properties used in the analysis are given in Appendix I.

Since the structure is symmetric about the x-y plane, it is necessary to consider only one half of the vessel, as shown in Fig. 2. The idealized model is composed of a mesh of 410 twenty-noded, three-dimensional isoparametric elements, divided into twenty-seven element groups for the stiffness analysis performed by the ADINA finite element code [4], using the isotropic thermo-elastic material model. The total number of nodes in the mesh is 2539.

3 THEORETICAL APPROACH

A mathematical description of the method appears in Appendix II - a brief description follows.

The method requires a number of distinct stress solutions to be formulated. Of these, at least one (σ_0) must satisfy the boundary loading and the remainder (σ_i) will be self-equilibrating sets. The stress at any time can be expressed as a weighted sum of the individual distributions, as follows

$$\sigma = \sigma_0 + \sum_{i=1}^{i=N} a_i \sigma_i \quad (1)$$

where a_i are time-dependent weighting parameters, and represent the unknowns in the problem. The σ_0 and σ_i are functions of space only.

A temperature-dependent Maxwell model representation in pseudo-time has been used, England and Allen [5], and this leads to a first order linear matrix differential equation in pseudo-time from which the a_i parameters of eq. (1) are determined. This equation has the form

$$[A][\dot{a}] + [B][a] + [C] = 0. \quad (2)$$

Substituting the a_i values of eq. (2) into eq. (1) yields the time-dependent stress solution.

4 NUMERICAL SOLUTION

The creep solution proceeds in two stages.

1 A standard finite element stiffness analysis is used to generate the stress solutions, σ_0 and σ_i .

2 A second program then optimizes the stress solutions of stage (1) according to the theory of Section 3, and Appendix II.

At least one σ_i (self-equilibrating distribution - SED), together with the σ_0 distribution, is required to obtain the input to stage (2). Experience has shown, however, that the minimum number of SEDs should not fall below two to retain accuracy of solution. Additional refinement can be achieved by increasing this number (Figs 3-5).

4.1 Stiffness Analysis

An elastic solution for the specified problem is generated using a standard finite element stiffness analysis. This solution becomes the σ_0 of eq. (1).

The SEDs may be obtained either from the difference between any two solutions corresponding to the same boundary loading and using different material properties, or from any thermal stress solution. These solutions are derived from the repeated use of the same finite element programs. For any analysis employing at least two SEDs for which one is taken to be the true thermal stress solution for the problem and one other represents the difference between the limiting steady-state and initial elastic solutions, the approximate transient creep solution is constrained to lie between the initial elastic and true steady-state solution.

4.2 Optimization Procedure

The stage (2) program draws on the stress solutions of stage (1) to form stress products, element by element. This is elaborated upon in Appendix II and is performed over the entire volume of the structure. The products formed represent the elements of [A], [B] and [C] matrices in eq. (2). Solving eq. (2) yields the a_i values, and hence the time-dependent stress solution can be obtained (eq. (1)).

5 RESULTS

The three-dimensional time-dependent stress distributions in the structure obtained by the minimum power method have been studied on many horizontal and vertical sections of the

vessel. Figs 3-6 show typical examples using two, three and four SEDs. Fig. 7 shows results taken from an axisymmetric PCRV analysis and compares a four SED approximate solution with the 'exact' solution taken from a time-step analysis incorporating many small time steps.

6 DISCUSSION

Fig. 7 reveals that when four SEDs are used in the approximate creep analysis, the results differ from the exact values by a minimal amount. Thus, Figs 3 and 4 illustrate convergence towards the 'exact' solution, as the number of SEDs is increased. Further evidence that significant changes occur by increasing the number of SEDs beyond two is furnished in Figs 5 and 6. Another feature of the results is that - independent of the number of SEDs used - the transient creep phase is bounded between the initial elastic solution and the SSL.

Returning to the specific example considered: the variations of stress in space and time and the stress concentrations near the roof penetrations and the roof-wall junction were found to be consistent with the geometry, loading and spatial temperature distribution. The general features of the results are also confirmed by a similar three-dimensional creep analysis of the roof portion of the vessel. In regions of the vessel far removed from zones of asymmetric geometry, the results show the expected axisymmetric behaviour.

Although a three-dimensional time-step creep analysis was not performed for the whole vessel, the cost of such an analysis was estimated to be approximately £40,000. For the minimum power analysis, the cost was £9530 with two SEDs and approximately £15,000 with four SEDs.

7 CONCLUSIONS

- 1 The method has been used successfully in the three-dimensional analysis of a PCRV.
- 2 It has the following advantages:
 - a it is relatively inexpensive and easy to use,
 - b accuracy can be increased or reduced at increased or reduced cost, and this is controlled by the user,
 - c stress outputs may be obtained at discrete times without the need to perform time-steps,
 - d the input data required by this method may be obtained from standard elastic analyses.
- 3 The total computer cost for the problem considered and using four SEDs was approximately 40 per cent of the estimated cost of the equivalent time-step solution. This cost fell as low as 25 per cent when only two SEDs were used.

ACKNOWLEDGEMENTS

This paper is presented by permission of the Director, National Engineering Laboratory, UK Department of Industry, and was sponsored by HM Nuclear Installations Inspectorate. It is (C) British Crown copyright.

REFERENCES

- 1 ENGLAND, G.L., "Steady-state stresses in concrete structures subjected to sustained temperatures and loads", *Nucl. Eng. Design*, 3, (1) 54-65, (2) 246-255 (1966).
- 2 ENGLAND, G.L., MacLEOD, J.S., "A direct method of structural analysis for creep in heated concrete structures", *Proceedings Fourth Int. Conf. on Structural Mechanics in Reactor Technology*, San Fransisco, USA, 1977, Paper H3/1.

- 3 SMITH, I.G., "Application of ADINA and ADINAT in the creep analysis of heated concrete structures", J. Computers and Structures, (in press).
- 4 BATHE, K.J., "ADINA - A finite element program for automatic dynamic incremental non-linear analysis", Report No 82448-1, Dept of Mechanical Engineering, Massachusetts Institute of Technology, 1975, (revised 1978).
- 5 ENGLAND, G.L., ALLEN, S.J., "The calculation of time-dependent stresses in PCPVs by an approximate method", Proceedings First Int. Conf. on Structural Mechanics in Reactor Technology, Berlin, Germany, 20-24 September 1971, Part H, pp 289-313.

A P P E N D I X I

Thermo-elastic analysis - material properties

T	19.5	70	°C
E	35.04×10^3	29.5925×10^3	MN/m ²
ν	0.2	0.2	
α	0.1×10^{-4}	0.1×10^{-4}	per °C

Reference temperature = 20°C.

Minimum power method analysis

Material to obey the uniaxial creep law:

$$\epsilon_c = 1.4505 \times 10^{-7} (T - 5) \sigma t^{0.32}.$$

Young's modulus and Poisson ratio were the same as for the thermo-elastic analysis.

A P P E N D I X I I

The computer program for the second stage of the numerical solution is based on the fact that the complementary power is a minimum, that is

$$\int \dot{\epsilon} \delta \sigma \, dv = 0 \quad (3)$$

where $\dot{\epsilon}$ is strain rate with respect to pseudo-time, t , and $\delta \sigma$ is any self-equilibrating stress variation and may be taken successively as σ_i for $i = 1$ to N in eq. (1). With a Maxwell material model when the elastic and creep Poisson ratios are equal, we obtain

$$[\dot{\epsilon}] = \{D/E + \phi(T)\}[V][\sigma] \quad (4)$$

where D is the differential operator d/dt and $\phi(T)$ the creep-temperature normalization function.

$$[V] = \begin{bmatrix} 1 & -\nu & -\nu & 0 & 0 & 0 \\ -\nu & 1 & -\nu & 0 & 0 & 0 \\ -\nu & -\nu & 1 & 0 & 0 & 0 \\ 0 & 0 & 0 & 2(1+\nu) & 0 & 0 \\ 0 & 0 & 0 & 0 & 2(1+\nu) & 0 \\ 0 & 0 & 0 & 0 & 0 & 2(1+\nu) \end{bmatrix} \quad [\sigma] = \begin{bmatrix} \sigma_x \\ \sigma_y \\ \sigma_z \\ \sigma_{xy} \\ \sigma_{yz} \\ \sigma_{zx} \end{bmatrix}$$

Substitution of σ from eq. (1) into eq. (4) leads to the strain rates in terms of a_i and their time derivatives and the spatial distributions of stress σ_0 and σ_i . Eq. (4) may be rewritten as

$$[\dot{\epsilon}] = \frac{[V]}{E} [[\sigma_1], [\sigma_2] \dots [\sigma_N]] \begin{bmatrix} \dot{a}_1 \\ | \\ \dot{a}_N \end{bmatrix} + \phi(T)[V][[\sigma_1] \dots [\sigma_N]] \begin{bmatrix} a_1 \\ | \\ a_N \end{bmatrix} + \phi(T)[V][[\sigma_0]]. \quad (5)$$

It then follows from eq. (3) that

$$0 = \int \dot{\epsilon} \delta \sigma \, dv = \int [\sigma_j]^T [\dot{\epsilon}] \, dv \quad \text{for } j = 1 \text{ to } N \quad (6)$$

because

$$\delta \sigma = \frac{\partial [\sigma]}{\partial a_j} = [\sigma_j].$$

After substitution of $[\dot{\epsilon}]$ from eq. (5), eq. (6) leads to the matrix differential eq. (2), ie

$$[A][\dot{a}] + [B][a] + [C] = 0.$$

The general terms of the matrices in this equation are

$$A_{rs} = \int 1/E [\sigma_r]^T [v] [\sigma_s] \, dv$$

$$B_{rs} = \int \phi(\tau) [\sigma_r]^T [v] [\sigma_s] \, dv$$

$$C_r = \int \phi(\tau) [\sigma_r]^T [v] [\sigma_0] \, dv.$$

To illustrate, in the above a contribution to A_{11} from one element would be

$$\left\{ \frac{\sigma_{1x}}{E} - \frac{\nu}{E} (\sigma_{1y} + \sigma_{1z}) \right\} \sigma_{1x} \, dv + \left\{ \frac{\sigma_{1y}}{E} - \frac{\nu}{E} (\sigma_{1x} + \sigma_{1z}) \right\} \sigma_{1y} \, dv + \left\{ \frac{\sigma_{1z}}{E} - \frac{\nu}{E} (\sigma_{1x} + \sigma_{1y}) \right\} \sigma_{1z} \, dv + \\ + \frac{2(1+\nu)}{E} \sigma_{1xy} \sigma_{1xy} \, dv + \frac{2(1+\nu)}{E} \sigma_{1yz} \sigma_{1yz} \, dv + \frac{2(1+\nu)}{E} \sigma_{1xz} \sigma_{1xz} \, dv.$$

Corresponding contributions from every other element in the structure would have to be added.

In the computer program, Gauss numerical integration was used to integrate the stress products over each element. The elements were transformed into cubes in ζ, η, ξ space and the integral of a function, eg the integrand of the expression for A_{rs} , is

$$I = \int_{-1}^1 \int_{-1}^1 \int_{-1}^1 f(\zeta, \eta, \xi) \, d\zeta, d\eta, d\xi = \sum_{i=1}^n \sum_{j=1}^n \sum_{m=1}^n H_i H_j H_m f(\zeta_i, \eta_j, \xi_m)$$

where H_i, H_j, H_m are Gauss coefficients and the summation is over all the Gauss points in the element. To arrive at the value of the integral in global coordinates, the contribution at each Gauss point is multiplied by the value of the determinant of the Jacobian at that point.

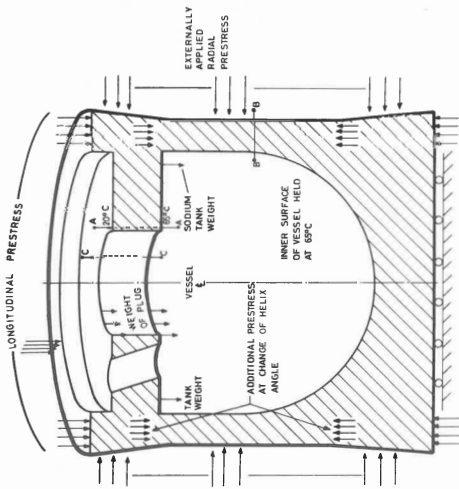
The solution of the matrix differential eq. (2) is

$$[a] = \exp\{-[A]^{-1}[B]t\} [K] - [B]^{-1}[C] \quad (7)$$

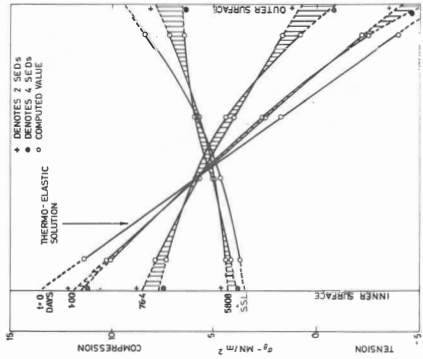
where $[K]$ is a vector of coefficients determined from the initial condition. When σ_0 represents the true elastic solution, it follows that $[a(0)] = 0$ and hence

$$[K] = [B]^{-1}[C].$$

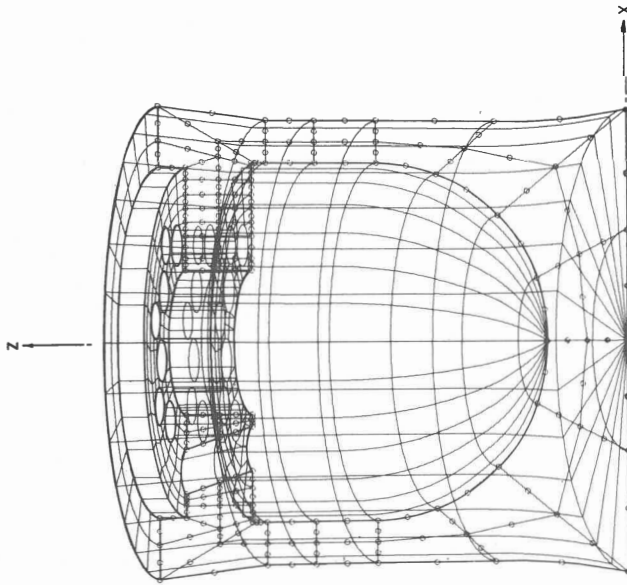
Substitution of $[a]$ into eq. (1) yields the time-dependent stress solution. Eq. (7) was solved numerically in the computer program by calculating $\exp\{-[A]^{-1}[B]t\}$ for a small value of time, t , from a series expansion, and checking that sufficient terms for the accuracy required had been taken. The sum of the series is the matrix $[Q]$ for time t . Then $[Q]^2, [Q]^4, [Q]^8$ etc correspond to $2t, 4t, 8t$ etc, and values of $[a]$ could be calculated from eq. (7) for these times. Double precision arithmetic was used for the solution of eq. (7).



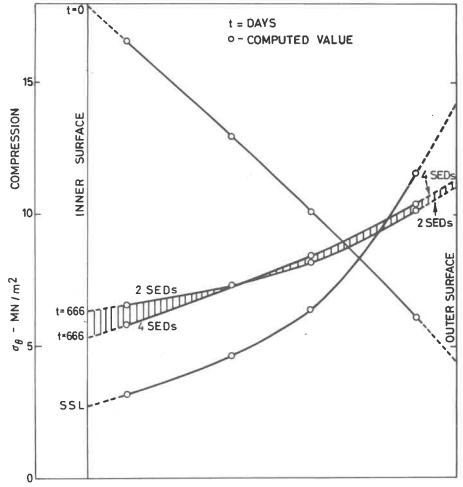
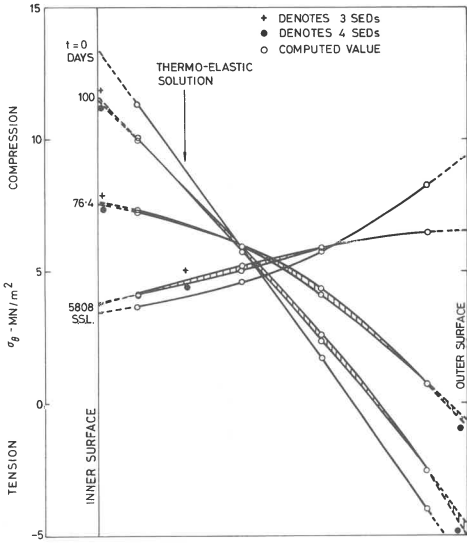
1 Vertical section of symmetric PCRV. Penetrations in roof section are omitted for simplicity



3 Circumferential stresses in wall section B-B; comparison of results using two and four SEDs

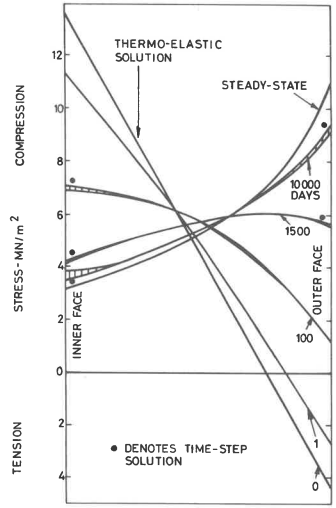
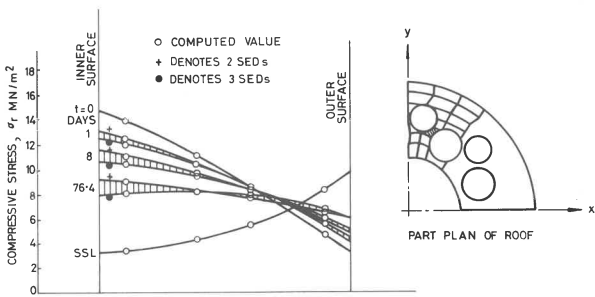


2 Details of finite element mesh for PCRV



4 Circumferential stresses in wall section B-B; comparison of results using three and four SEDs

5 Circumferential stresses in roof section A-A; comparison of results using two and four SEDs



6 Radial stresses in roof section C-C; comparison of results using two and three SEDs. (CC is vertical through shaded element)

7 Axisymmetric analysis. Circumferential stresses in wall section B-B; comparison of time-step and approximate solutions using four SEDs.